North Atlantic atmospheric circulation indices: links with summer and winter temperature and precipitation in north-west Europe, including persistence and variability

Received: 7 June 2023 | Revised: 22 November 2023 | Accepted: 29 December 2023

DOI: 10.1002/joc.8364

RESEARCH ARTICLE

International Journal of Climatology RMetS

North Atlantic atmospheric circulation indices: Links with summer and winter temperature and precipitation in north-west Europe, including persistence and variability

Ian Simpson[1] | **Edward Hanna**[1] | **Laura Baker**[2] | **Yiming Sun**[3] | **Hua-Liang Wei**[3]

[1]Department of Geography and Lincoln Climate Research Group, College of Science, University of Lincoln, Lincoln, UK

[2]National Centre for Atmospheric Science, Department of Meteorology, University of Reading, Reading, UK

[3]Department of Automatic Control and Systems Engineering, University of Sheffield, Sheffield, UK

Correspondence
Ian Simpson, Department of Geography and Lincoln Climate Research Group, College of Science, University of Lincoln, Lincoln, UK.
Email: isimpson@lincoln.ac.uk

Funding information
Natural Environment Research Council, Grant/Award Number: NE/V001787/1

Abstract

Variability in seasonal weather in north-west Europe is substantially determined by jet stream variability. The North Atlantic Oscillation (NAO) has been well studied as a key representation of this jet stream variability, but other circulation indices are also important. Here the first three principal component empirical orthogonal functions (EOFs) of 500 hPa geopotential height (GPH), which broadly correspond to the NAO, the East Atlantic pattern (EA) and Scandinavian pattern (SCA), as well as jet speed and latitude, are correlated with temperature and precipitation anomalies over Europe with a focus on north-west Europe, as well as measures of persistence and variability. In high summer (July and August), all three of the principal EOFs are significantly correlated with extreme temperatures in large areas of northern Europe. In winter, for much of north-west Europe, both temperatures and precipitation are positively correlated with the jet speed, and precipitation is negatively correlated with EOF3. There is some non-stationarity in some of the relationships, notably between winter precipitation and EOF1, and between July/August precipitation and EOF2. In addition to single variate correlations, multiple correlation coefficients are also used to determine areas of significant correlation when combining two or three of the circulation indices. The multiple correlation analyses show that combining the three EOFs produces significant correlations with temperature and precipitation over much of Europe. These analyses provide scope for using seasonal forecasts to predict likely temperature and precipitation anomalies based on predicting the atmospheric circulation anomalies and downscaling them. Improved seasonal forecasts of temperature and precipitation, including persistence and variability, will be useful to a number of users, such as agrifood, transport, energy supply and insurance.

KEYWORDS
EOF, jet stream, north-west Europe, precipitation, seasonal forecasting, temperature

1 | INTRODUCTION

Variability in the weather in north-west Europe is substantially determined by atmospheric circulation. In winter, the leading empirical orthogonal function of the Northern Hemisphere pressure field is the North Atlantic Oscillation (NAO: Hurrell et al., 2003, Hurrell & Deser, 2009). The NAO is traditionally defined as the normalized sea-level pressure (SLP) difference between the Azores and Iceland (Kendon et al., 2022), although sometimes Lisbon or Gibraltar is used instead of the Azores (Hall & Hanna, 2018). A positive winter NAO sees a large pressure difference between high pressure over the Azores and low pressure over Iceland, sending low-pressure systems north-eastwards and increasing storm activity in northern Europe, while decreasing it in southern Europe (Hurrell & Deser, 2009). In the UK, a positive winter NAO is linked with mild, wet winters, while a negative NAO tends to be linked with cold, dry winters (Kendon et al., 2022). The NAO accounts strongly for winter precipitation in the north and west of the UK, but not in the south and east (Hall & Hanna, 2018).

The jet stream generally takes a more northerly track in the summer months, and this is reflected by behaviour of the summer NAO (Folland et al., 2009), when a positive summer NAO is associated with high pressure ridging from the Azores towards Britain and Scandinavia, bringing predominantly warm and dry weather to those regions, and low pressure over Iceland. The summer NAO (Folland et al., 2009) has been studied chiefly in relation to high summer (July and August), on the basis that its temporal behaviour in July and August is closely correlated, but not with June. However, a similar NAO pattern is also evident for June (Barnston & Livezey, 1987).

Although the NAO is the first EOF of SLP or 500 hPa geopotential height over the North Atlantic/north-west Europe region, two other lower-order EOFs also account for a significant amount of variability. The second EOF, the East Atlantic pattern (EA), is a north–south dipole SLP or 500 hPa GPH anomaly that is shifted south-eastwards of the NAO pattern (Thornton et al., 2023). When combined with the NAO, the EA explains a higher percentage of variability than the NAO alone (Woollings & Blackburn, 2012). A positive EA is associated with a low-pressure anomaly in the eastern North Atlantic. For example, the high rainfalls of the UK winters of 2013/14 and 2015/16 were associated with a combination of a positive NAO and a positive EA, while the winter of 2014/15, which was relatively dry in the south and east of Britain, also had a positive NAO but a negative EA (Hall & Hanna, 2018).

The third principal EOF of sea-level pressure variability in this region is the Scandinavian pattern, as first identified by Barnston and Livezey (1987). Traditional measures of SCA have a low pressure anomaly to the west and south-west of Britain and a high pressure anomaly over Scandinavia (Bueh & Nakamura, 2007), and are associated with above-average winter precipitation in south-western Europe and below-average precipitation in Scandinavia and along the Arctic coast of Eurasia.

Thus, as discussed by Hall and Hanna (2018), while seasonal forecasts often focus on the NAO, it is useful to consider the EA and SCA as well, especially in cases such as the aforementioned winters of 2013/14 and 2015/16, where the positive EA as well as the positive NAO played a major role in the very wet weather that was experienced over much of the UK. Hall and Hanna (2018) related three principal EOFs of SLP that correspond approximately to the NAO, EA and SCA to winter and summer temperature and precipitation patterns over the UK.

This paper extends this previous work by examining the relationships between the three principal EOFs, jet speed and latitude and temperature and precipitation patterns over the much larger spatial scale of Europe and the east Atlantic sector, focusing chiefly on north-west Europe. Another aim is to determine relationships between large-scale circulation patterns and the persistence and variability of surface air temperature and precipitation, and to identify areas where these differ in sign and/or strength from the relationships with maximum and minimum temperature and total precipitation.

Dynamical models have shown significant skill in predicting the winter NAO, with for example Scaife et al. (2014) finding that the ensemble mean signal in the Met Office GloSea5 seasonal prediction model (MacLachlan et al., 2015) showed a correlation of 0.62 with the observed winter NAO. Tropical forcings such as ENSO (Ineson & Scaife, 2009), the Indian Ocean Dipole (Hardiman et al., 2020) and Pacific SSTs (Huntingford et al., 2014) have been found to be important sources of NAO predictability. However, while dynamical forecasts are sensitive to tropical forcings, they show evidence of being relatively insensitive to Arctic variability (Cohen et al., 2019) and show lower forecast skill in summer, when tropical forcing is weaker, than in winter (Hall et al., 2015). Furthermore, using forecasts of temperature

and, especially, precipitation directly from dynamical seasonal forecasts tends to produce low skill since the dynamical models have many local biases (Haiden & Trentmann, 2015). This motivates approaches such as this one, where forecasts of modes of variability (which tend to be more skilful) can be used with the observed relationships to temperature and precipitation to provide forecasts. Preliminary results from Sun et al. (submitted), suggest that NARMAX machine learning methods are capable of predicting summer NAO, EA and SCA and winter EA and SCA with considerable skill, as well as the winter NAO (Hall et al., 2019), and this increased skill means that a systemic analysis of the relationships between winter and summer NAO, EA and SCA and regional temperature and precipitation may be of greater use for forecasters and the general public.

In this paper we analyse the relationships between the three principal EOFs of atmospheric circulation variability and temperature and precipitation patterns across Europe, for winter (DJF), June and for high summer (JA), focusing especially on north-west Europe. Section 2 discusses the data used for this analysis, Section 3 outlines the methods used, and Section 4 presents the results, using 30 km ERA5 reanalysis data for Europe and then using 5 km HadUK-Grid data for the UK, as a higher resolution case study. Section 5 contains a discussion of the results, and Section 6 provides a summary of the key conclusions.

2 | DATA

Three principal empirical orthogonal functions (EOFs) of European and North Atlantic atmospheric circulation variability were generated using monthly averaged detrended 500 hPa GPH data from the European Centre for Medium-Range Forecasts (ECMWF) ERA5 reanalysis (Hersbach et al., 2020), combined with the Python EOFs package (Dawson, 2016), covering the period 1950–2021 and applied to individual months and seasons independently. These correspond closely to the North Atlantic Oscillation (NAO), East Atlantic pattern (EA) and Scandinavian pattern (SCA). We obtained ERA5 500 hPa geopotential heights from the Copernicus Climate Data Store.

Maps for the winter and summer EOFs are shown in Figure 1. The three winter EOFs (top row) are largely similar to the EOFs obtained by Hall and Hanna (2018) but, possibly due to the different reanalysis datasets used 20CRv2 and ERA-Interim in that study and/or methodological differences in calculating EOFs, also show some notable differences. However, Figure S1 suggests that methodological differences may be more important, as the principal EOFs do not change substantially in successive 30-year periods ending in '0' from 1961–1990 to 1991–2020, although there are small changes in the positioning of the regional anomaly centres.

For example, the winter Scandinavian pattern has the high GPH anomaly further west than the SLP anomaly in Hall and Hanna (2018), centred to the north and north-east of the British Isles, while winter EOF1 has the low height anomaly centred to the south of Greenland, rather than over Iceland. For the summer EOFs, June is shown separately from high summer (July/August) as using the full June/July/August data generates a poorly defined pattern for EOF1, while the typical summer NAO pattern appears as EOF2. This is consistent with previous analysis, for example, (Folland et al., 2009) which suggests there is a strong summer NAO signal that characterizes July and August, while the summer NAO behaves differently during June. For June and for July/August, EOF1 is consistent with the Folland et al. (2009) summer NAO, which has a weaker negative GPH anomaly over Greenland and Iceland which is shifted to the north of its winter position, and a high height anomaly extending through Britain and Scandinavia.

The percentage of covariance that the three principal EOFs account for is given in Table 1. The percentages for June and for July/August are comparable to those of Hall and Hanna (2018), but for winter EOF1 accounts for a smaller percentage of variability (30.2%, as opposed to 48.1% in Hall & Hanna, 2018).

In addition to using the three principal EOFs of atmospheric circulation variability, monthly time series of North Atlantic jet speed and latitude were derived from the ERA5 reanalysis based on Woollings (2010), based on the North Atlantic region (16–76° N, 60–0° W) and seasonally averaged, weighted by the number of days in each month. The maximum zonal mean is given as the jet speed for a given day, while the latitude value at which it occurs is given as the jet latitude. Note that in some cases the EOF time series are correlated with those of jet speed and latitude, for example, over the period 1956–2021, winter EOF1 had a correlation of 0.62 with jet latitude, and 0.46 with jet speed.

Hourly temperature data and precipitation data were obtained via the ERA5 reanalysis at 30 km resolution and converted to daily maximum and minimum temperatures and daily precipitation totals using CDO from the Copernicus Climate Change Service CDS Toolbox. These data were used to conduct a general analysis of the relationships between atmospheric circulation variability and temperature and precipitation persistence and variability for Europe and the eastern North Atlantic, focusing on north-west Europe. In addition, Met Office HadUK-Grid (Hollis et al., 2019) daily maximum and minimum temperature and precipitation data were obtained at 5 km resolution, covering the UK only, to provide a higher-resolution case

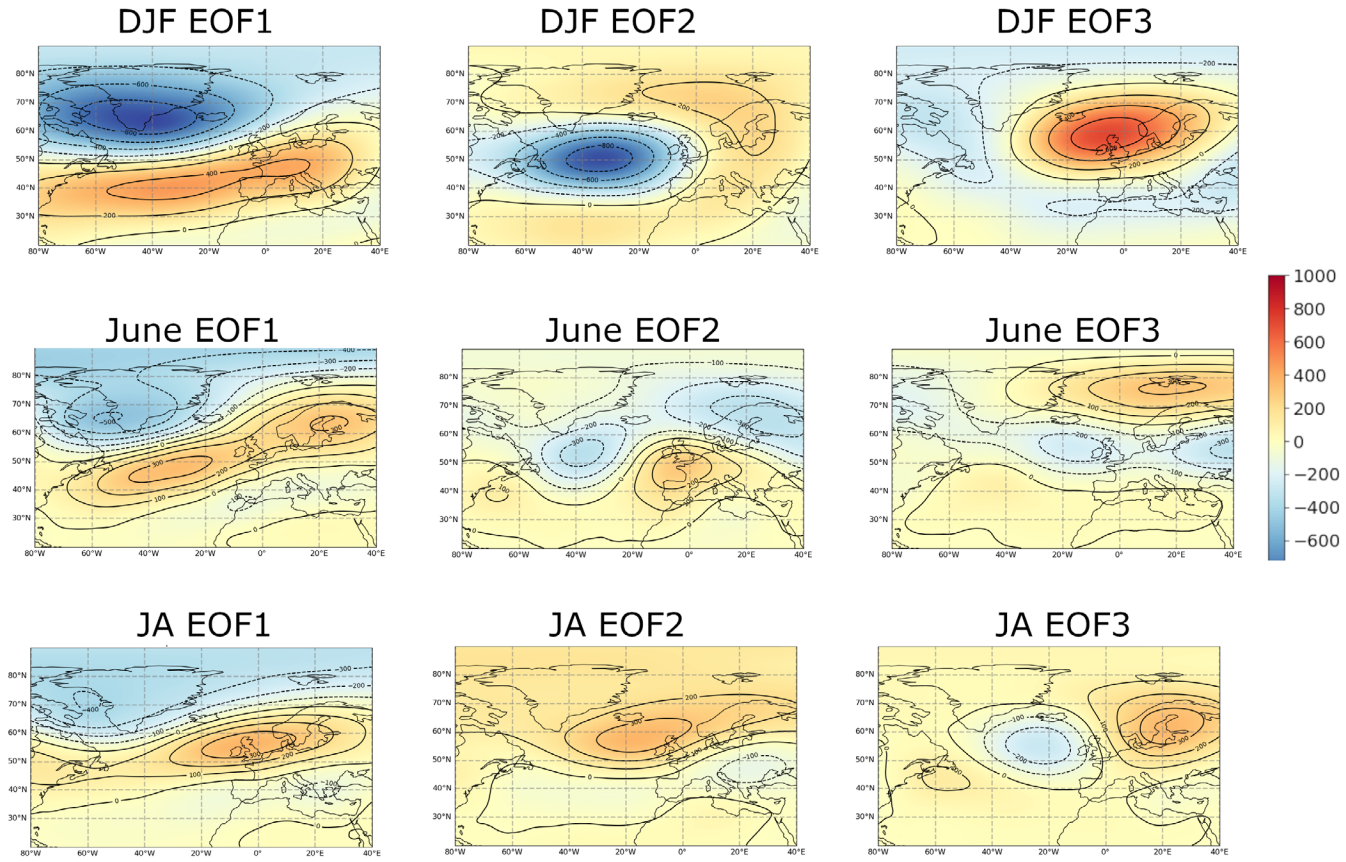

FIGURE 1 The three primary EOFs of atmospheric circulation variability (at the 500 hPa geopotential height level) from ERA5 reanalysis based on 1950–2021 for winter (December/January/February, left), June (middle) and high summer (July and August, right). EOFs are applied to these months and seasons independently. [Colour figure can be viewed at wileyonlinelibrary.com]

TABLE 1 Percentage of covariance that is explained by the three principal EOFs shown in Figure 1.

	Winter	June	July/August
EOF1	30.2%	28.9%	24.8%
EOF2	18.6%	14.7%	14.7%
EOF3	13.0%	8.8%	10.9%

study that can provide more insights into, for example, topographical and coastal effects. Observations in all datasets are linearly detrended with the aim of isolating the association between atmospheric circulation and temperatures and rainfall and reducing the risk of biases being introduced due to long-term trends. Winters are denoted by the year of the January.

3 | METHODS

Pearson correlation coefficients were generated to compare seasonal temperature and precipitation with the three principal EOFs, as well as jet speed and jet latitude. Linear regressions were used to generate estimated p-values, with significant correlations defined as correlations with *p*-values below 0.05 (95% confidence). As well as maximum temperature, minimum temperature, mean temperature and mean total precipitation, a number of persistence and variability indices were also used, drawing upon and sometimes adapted from the ETCCDI Climate Change Indices (Karl et al., 1999; Peterson et al., 2001). The indices that were chosen for maximum and minimum temperature and for precipitation are provided in Table 2.

It is useful to assess the combined relationship of the EOFs and jet speed and latitude with temperature and precipitation. Thus, multivariate regressions were also generated between combinations of the EOFs and temperature and precipitation, to determine the multiple correlation coefficients from the adjusted R-squared values, to determine whether particular combinations of EOFs are particularly strongly associated with variations in temperature and precipitation and associated indices of persistence and variability.

The 30 km gridded temperature and precipitation data from the ERA5 reanalysis were correlated with individual

TABLE 2 List of measures of persistence and variability used for temperature and precipitation analysis. Summer indices are used both for June and for July/August.

Summer maximum temperature	Summer minimum temperature	Winter maximum temperature	Winter minimum temperature	Precipitation (both seasons)
Max daily	Max daily	Max daily	Max daily	Max daily
Mean daily	Mean daily	Mean daily	Mean daily	Mean daily
Min daily	Min daily	Min daily	Min daily	Days with total precipitation above 5 mm
Days above 25C	Days above 18C (July/August) or 16C (June)	Ice days (max below 0C)	Air frosts (min below 0C)	Days above the 90th percentile
Days above the 90th percentile	Days above the 90th percentile	Days above the 90th percentile	Days above the 90th percentile	Consecutive dry days (<0.2 mm)
Consecutive days above the 80th percentile	Consecutive days above the 80th percentile	Consecutive days below the 20th percentile	Consecutive days below the 20th percentile	Consecutive wet days (≥1 mm)
Days below the 10th percentile	Days below the 10th percentile	Days below the 10th percentile	Days below the 10th percentile	Days below the 10th percentile
Standard deviation	Standard deviation	Standard deviation	Standard deviation	Standard deviation

EOFs and with jet speed and latitude, with the aim of determining areas of significant correlation that are potentially worth identifying on the basis of forecasts of the principal EOFs and improving our understanding of how atmospheric circulation affects temperature and precipitation anomalies. For each set of results, results from 30-year periods ending in '0', from 1961–1990 to 1991–2020, were computed, to determine whether relationships between atmospheric circulation and temperature and precipitation have been shifting as global and regional climates have transitioned from the 1960s through to the 2020s. This work expands upon previous work by Hall and Hanna (2018), who only considered two fixed time periods of 1951–2014 and 1979/1980–2016 based on the older ERA Interim reanalysis, but the EOFs generated for this study have some small differences as discussed in Section 2. Unlike previous studies, multivariate correlations are assessed in addition to single-variate correlations, to give indications as to which combinations of the three principal EOFs are particularly strongly correlated with temperature and precipitation in north-west Europe. In the case of summer, the EOFs have been split into June and July/August, for reasons that were discussed in Section 2. A follow-up analysis was conducted using the Met Office HadUK-Grid gridded datasets (Hollis et al., 2019), containing maximum and minimum temperature and precipitation over the UK at 5 km resolution.

4 | RESULTS

In this section, only significant correlations ($p < 0.05$) are discussed unless explicitly stated otherwise. For each season, the three principal EOFs, jet speed and jet latitude are compared with temperature and precipitation patterns over Europe in Section 4.1, and then over the UK in Section 4.2. The various temperature and precipitation indices in Table 2 are analysed. To synthesize results, the strongest correlations and most important results are provided in the main figures and discussed in detail. Other findings are discussed in less detail and shown in the Supporting Information figures.

4.1 | ERA5 correlations

4.1.1 | Summer temperatures

In the case of high summer (July and August), all three of the principal EOFs are correlated with high maximum and minimum temperatures over parts of northern Europe. Figure 2 shows the correlations with daily maximum temperatures above the 90th percentile, corresponding to extreme hot days. These are positively linked with EOF1 (Figure 2a) and EOF2 (Figure 2b) over large areas of north-west Europe, with correlations of 0.6 to 0.7 with EOF1 in parts of Britain and Norway, but negative correlations are observed in parts of south-east Europe. They are also positively correlated with EOF3 (Figure 2c) in most of central and northern Europe but not Britain. This suggests that accurate predictions of the three EOFs will help us to predict the likelihood of extreme hot weather in the north and north-west of Europe in July and August. Jet stream forecasts are less likely to be useful guides, as there are

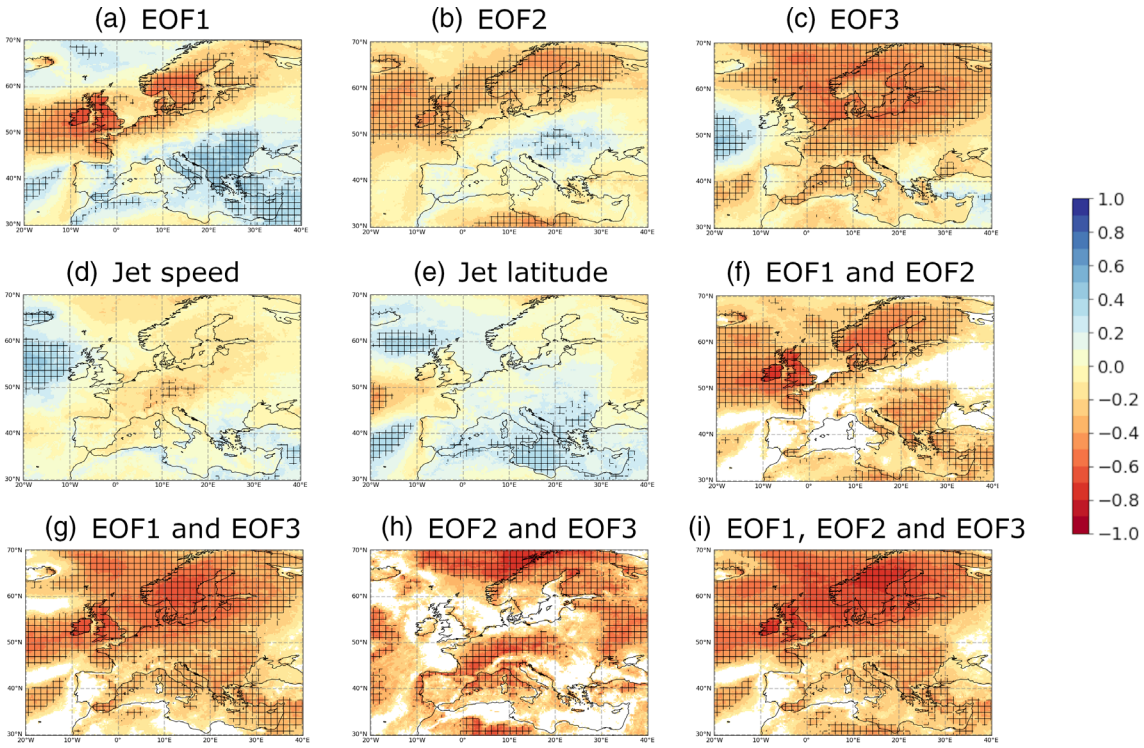

FIGURE 2 Correlations with high summer (July/August) occurrences of daily maximum temperature above the 90th percentile, indicating links with extreme hot days, over the period 1961–2021. Hatched areas indicate correlations that are significant at $p < 0.05$. [Colour figure can be viewed at wileyonlinelibrary.com]

few areas of significant correlation with jet speed (Figure 2d) or jet latitude (Figure 2e).

Other maximum temperature indices defined in Table 2 (not shown) typically show similar correlation patterns to maximum temperatures above the 90th percentile, including the mean maximum. However, consecutive days above the 80th percentile (indicating persistent hot spells) show weaker correlations in most cases, although there is a significant positive association between EOF1 and persistent hot spells in Britain and Norway. Britain and Scandinavia see a stronger positive link between EOF2 and extreme hot days (Figure 2b) than with the seasonal or monthly mean daily maximum temperature. Days over 25°C are significantly correlated with EOF1 in southern Britain, southern Scandinavia, northern France, the Netherlands and Denmark, but not with EOF2 or EOF3. Days below the 10th percentile, indicating unseasonably cool weather, are not strongly correlated with EOF2 in most regions, but show a significant negative correlation with EOF3 in most parts of central and northern Europe, and with EOF1 over the British Isles.

Multiple linear regressions of EOF1, EOF2 and/or EOF3 result in particularly strong correlations (around 0.6–0.7) with summer maximum temperatures over much of northern Europe (see Figure 2f–i). Relationships with summer minimum temperatures (not shown) are similar.

For June, correlations between the three EOFs and daily maximum temperatures above the 90th percentile are generally lower than the correlations with monthly mean maximum temperatures. Thus, correlations between mean maximum temperatures and the EOFs and jet speed and latitude are shown in Figure S2. EOF1 is positively correlated with mean maximum temperatures over most of Britain and Scandinavia (Figure S2a). EOF2 (Figure S2b) shows a positive correlation with mean maximum temperature over much of western Europe (France and Spain as well as Britain), while EOF3 (Figure S2c) is negatively correlated with mean maximum temperatures in western Britain. Again, there are few significant relationships between jet speed and jet latitude and temperature (Figure S2d,e). There are also few significant correlations between the EOFs and temperature and precipitation in central and eastern Europe. In most cases, the strength of these correlations has reduced for the latest period (1991–2020, not shown), with a reduction in the areas where they are significant, with the primary exception of maximum temperatures above the 90th percentile and EOF1, which have correlations of 0.6–0.7 over most parts of the British Isles during the period 1991–2020.

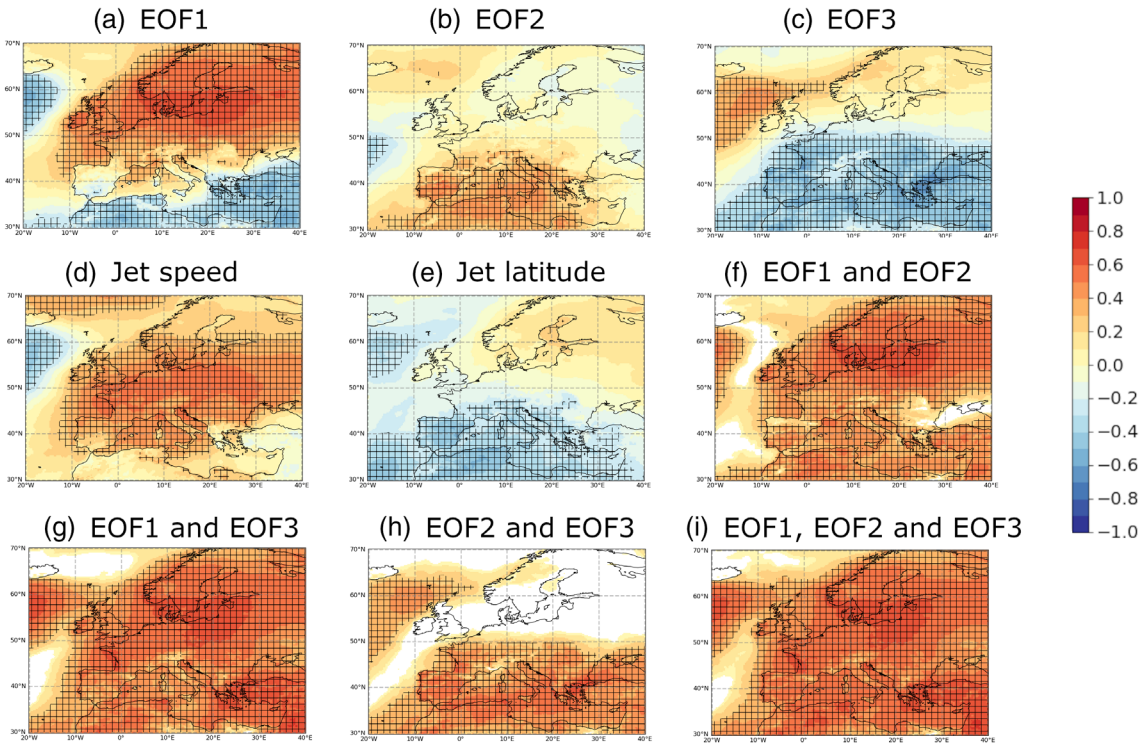

FIGURE 3 Correlations with mean winter minimum temperature over the period 1961–2021. Hatched areas indicate correlations that are significant at $p < 0.05$. [Colour figure can be viewed at wileyonlinelibrary.com]

The multiple correlation coefficients for June (Figure S2f–i) generate less widespread positive correlations than the July/August ones, but nonetheless the combination of EOF1 and EOF2 are significantly correlated with June temperatures over the British Isles, France and Spain. Correlations (around 0.7–0.8) are highest over Scandinavia, which arises from the combination of a strong positive correlation with EOF1 and a strong negative correlation with EOF2. The EOFs produce less widespread significant correlations with June extreme maximum temperature than June mean maximum temperature (Figure S5), reflecting the tendency for June extremes to be less well captured by the EOFs than mean maximum and minimum temperature.

Mean minimum temperatures broadly show the same correlation patterns as maximum temperatures. In June, correlations are generally weaker than for maximum temperatures, except in the case of EOF2 in western Europe. The standard deviation of June minimum temperatures is significantly negatively correlated with June EOF3 and jet speed in western Britain, pointing towards a negative association between jet speed and cyclonic conditions (EOF3 is linked with low heights in western Britain) and minimum temperature variability. July/August minimum temperatures also showed similar, but weaker, correlations in most cases, but with a comparably strong positive link with EOF3 in Scandinavia and northern Europe.

4.1.2 | Winter temperatures

Both mean maximum (shown in Figure S3) and mean minimum temperatures (shown in Figure 3) showed a positive correlation with EOF1 and winter jet speed over most of Europe. However, in parts of southern Europe including Spain, while maximum temperatures (Figure S3a) are significantly correlated with EOF1, minimum temperatures are not (Figure 3a), suggesting an association with warm days but relatively cool nights, consistent with anticyclonic and clear conditions with light winds. The strongest positive correlations between EOF1 and both maximum and minimum temperatures are found in northern Europe, while it is central Europe which sees the strongest link between winter temperature and jet speed. This perhaps reflects an association between high jet speeds and stronger westerlies in central as well as northern Europe.

EOF2 is linked with high winter minimum temperatures in southern and south-western Europe, particularly Spain and Italy (Figure 3b), while jet latitude is negatively linked with winter minimum temperatures in the same regions. EOF3 (Figure 3c) is linked with low winter maximum and minimum temperatures in central and southern Europe. This reflects the fact that EOF3 has the high GPH anomaly centred over northern Britain and the North Sea rather than Scandinavia (as per the

standard Scandinavian pattern), sending cold easterly winds into central and southern Europe rather than towards Britain.

While EOF1 is linked with daily temperatures above the 90th percentile in most parts of Europe, especially Scandinavia and eastern Europe, the correlations are generally lower than with mean temperature and not significant over as large an area (not shown). There are strong negative correlations with cold spells (as measured by consecutive days below the 20th percentile) and with extreme cold days (days below the 10th percentile). EOF1 and to a lesser extent jet speed are negatively linked with the standard deviation of minimum temperatures (not shown) in most parts of Europe, and of maximum temperatures in western Britain, Norway and Sweden.

The multiple correlation coefficients with mean seasonal winter daily minimum temperature (Figure 3f–i) tend to be dominated by the EOF1 signal, reflecting the strong positive correlations between the NAO and winter temperature in northern and north-western Europe. In southern Europe, they also reflect the negative relationship between winter temperatures and EOF3.

Taken together, these results suggest that EOF1 is more strongly linked with a lack of low daily winter temperatures than with unusually high daily temperatures, and with relatively limited temperature variability. These results are broadly consistent with previous studies of the winter NAO, which is encouraging as it suggests that EOF1 does correspond well with station-based measures of the NAO which use the SLP difference between the Azores and Iceland. EOFs 2 and 3 have potential to be useful predictors of winter temperatures in parts of southern Europe, particularly Spain.

4.1.3 | Summer precipitation

July/August precipitation (Figure S4) is inversely correlated with EOF1 over Britain, Scandinavia and the Netherlands, and positively correlated with EOF1 around the Mediterranean Sea. EOF1 is also positively linked with a high standard deviation in precipitation (not shown) over the dry areas, and less strongly linked with extreme low values and lack of wet days. This may be because dry anticyclonic weather can produce localized thundery downpours.

EOF2 is negatively correlated with July/August precipitation over most of western Britain (Figure S4b), most likely because this EOF features a high GPH anomaly to the north-west of Britain. However, this relationship has declined for the most recent 30-year period (1991–2020) (Figure S9). The other indices show generally weaker relationships with July/August precipitation, but jet speed is positively correlated with precipitation in north-west Scotland, and jet latitude is negatively correlated with precipitation in southern Britain.

Multiple correlation coefficients for July/August precipitation (Figure S4f–i) are particularly strong in western Britain and in southern Scandinavia, reflecting a strong likelihood of dry summer weather in western Britain when a positive summer NAO is combined with a high SLP anomaly in the eastern North Atlantic. The EOF1/EOF3 multiple correlation coefficients are dominated by the dry signal from EOF1, while the EOF2/EOF3 ones show few significant correlations for north-west Europe.

June precipitation (Figure 4) is also negatively correlated with EOF1 (Figure 4a) in Britain and southern Scandinavia and the Netherlands, and with EOF2 (Figure 4b) in the southern half of Britain and most of central Europe including France. Again, these links with drier weather are generally weaker when considering extreme high precipitation, both using daily occurrences above the 90th percentile and daily totals above 5 mm. The exception is the link between EOF1 and the British Isles, which, unlike the July/August NAO, also shows a strong negative link with high daily precipitation totals in Britain (not shown). June precipitation is positively linked with EOF3 (Figure 4c) in western and northern Britain. Jet speed is not significantly correlated with June precipitation but jet latitude is negatively correlated with precipitation in parts of France and the southern half of Britain but is positively correlated in extreme northern Scotland and along the west coast of Norway.

The June multiple correlations (Figure 4f–i) are particularly strong over the British Isles when combining EOF1 and EOF2, reaching around 0.7 in parts of the south, pointing to a strong tendency for dry weather in June when a positive summer NAO is combined with an above average tendency for above-average heights over central Europe and a trough in the eastern North Atlantic.

4.1.4 | Winter precipitation

Correlations between the EOFs, jet speed and latitude and days with over 5 mm of precipitation, indicating very wet winter days, are shown in Figure 5. EOF1 (Figure 5a) shows the typical positive NAO correlation with days with over 5 mm of precipitation in the west of Scotland and Ireland, as well as much of western and northern Scandinavia, and a negative correlation over much of southern Europe. Jet speed (Figure 5d) shows similar correlations to EOF1, but with less of a rain shadow effect to the east of high ground, resulting in more generally high correlations in Britain, the Netherlands and southern Scandinavia.

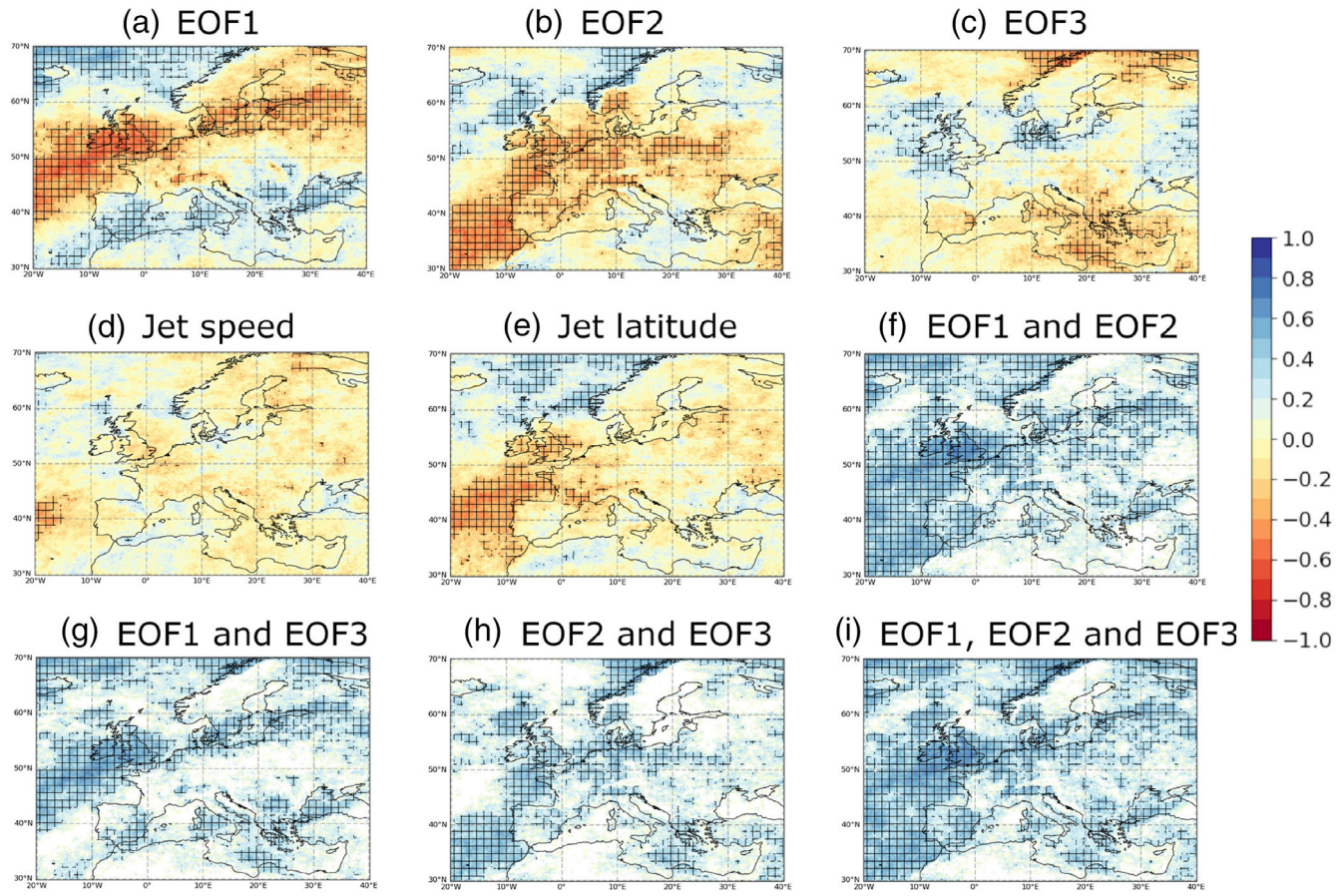

FIGURE 4 Correlations with June mean precipitation over the period 1961–2021. Hatched areas indicate correlations that are significant at $p < 0.05$. [Colour figure can be viewed at wileyonlinelibrary.com]

EOF2 (Figure 5b, corresponding to the winter East Atlantic pattern) has a positive link with precipitation in southern Britain, western France and much of Spain. EOF3 is negatively linked with winter precipitation across much of northern Europe, especially north-western Europe, which is linked with the high GPH anomaly centred over northern Britain and the North Sea.

Correlations between EOF1 and consecutive wet days (not shown) are lower than for mean precipitation (though still significant over large areas of northern Europe) but correlations with extreme high daily precipitation totals (Figure 5) are similar to those for mean precipitation, suggesting that a positive NAO is associated with frequent precipitation but not so much with long runs of wet days, which is consistent with active westerly types bringing drier interludes in between frontal systems. The standard deviation of precipitation (not shown) is positively correlated with jet speed in most parts of north-western Europe, implying that a faster jet results in greater daily precipitation variability.

Winter multiple correlation coefficients (Figure 5f–i) between EOF2 and EOF3, and between EOF1 and EOF3, are dominated by the negative correlations between EOF3 and winter precipitation. The combination of EOF1 and EOF2 is linked with above-average precipitation in southern as well as western Britain, but not in north-eastern Britain. Thus, a combination of positive values for EOFs 1 and 2 and a negative value for EOF3 would suggest a very wet winter over the British Isles, especially for western and southern Britain.

The results in Figure 6 show evidence of winters with a positive NAO and/or a strong jet stream becoming wetter in western Britain relative to winters with other circulation types with time, but rather than a gradual shift, a step-change has occurred between 1971–2000 and 1981–2010. For the two most recent periods, the positive correlations in northern Scandinavia have declined and were no longer significant at many grid boxes over 1991–2020.

A summary of the main results of this section is presented in Table 3.

4.2 | HadUK-Grid correlations

4.2.1 | Summer temperature

The higher spatial resolution of HadUK-Grid data causes some regional variations in the relationships with the EOFs to be more apparent, though broadly the

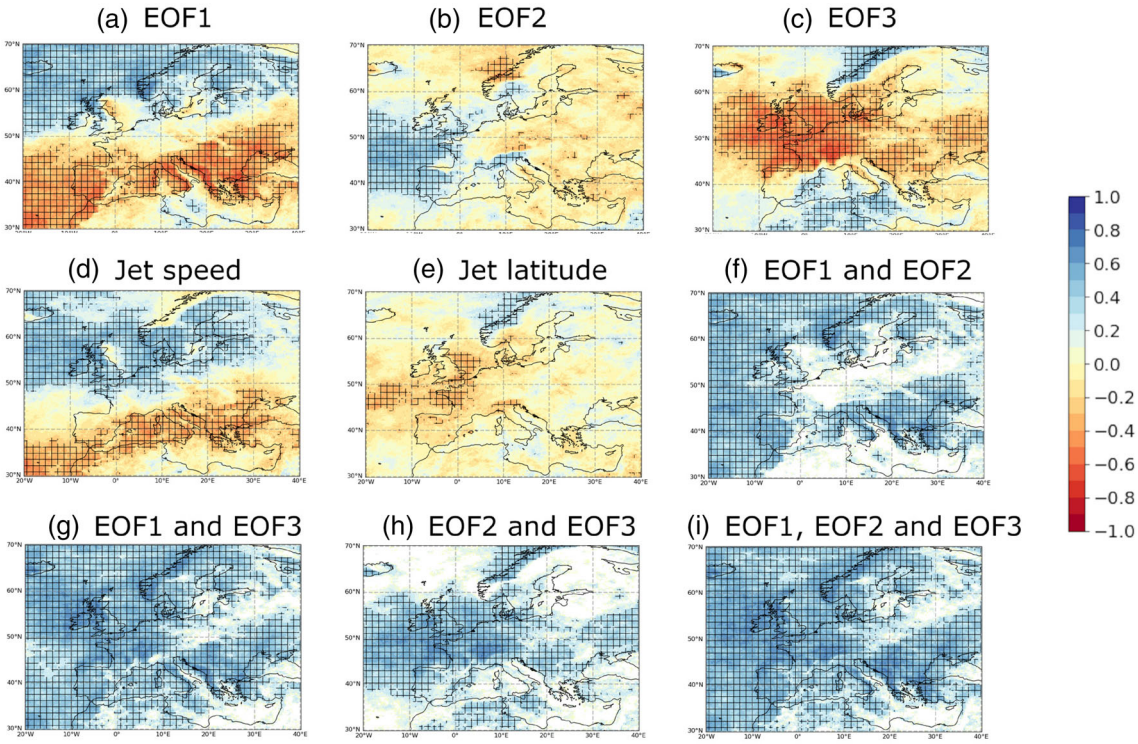

FIGURE 5 Correlations with very wet winter days (over 5 mm precipitation) over the period 1961–2021. Hatched areas indicate correlations that are significant at $p < 0.05$. The colour scale is reversed for precipitation. [Colour figure can be viewed at wileyonlinelibrary.com]

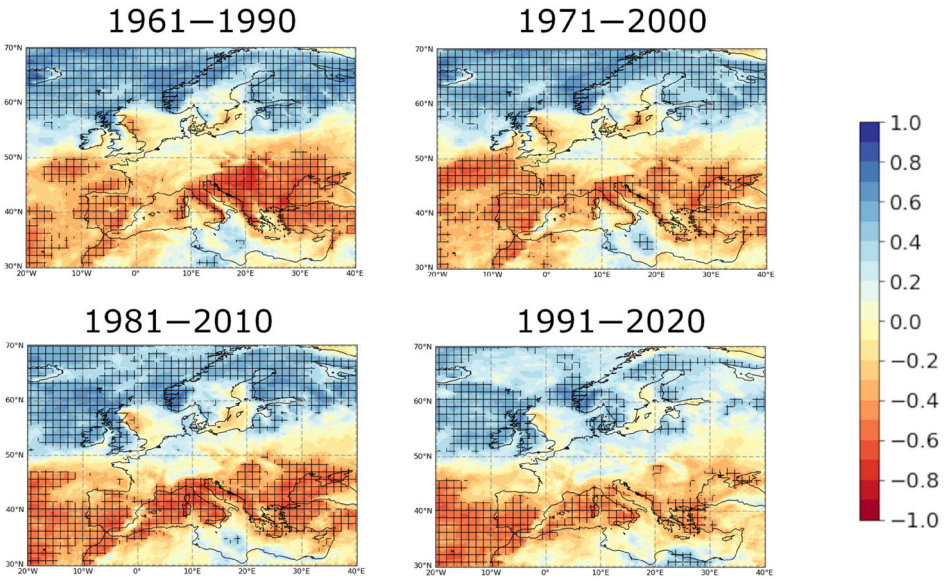

FIGURE 6 Correlations between mean winter precipitation and EOF1 for each successive 30 year period ending in '0'. Hatched areas indicate correlations that are significant at $p < 0.05$. [Colour figure can be viewed at wileyonlinelibrary.com]

correlation patterns are much the same as those observed using ERA5 data. The regions of the UK that are referenced in the text are given in Figure S10.

Correlations between the three principal EOFs and maximum temperatures above the 90th percentile for July/August are shown in Figure 7. For June, as in the ERA5 analysis, the correlations with maximum temperatures above the 90th percentile are generally lower and less widely significant than with mean maximum temperatures, and so the correlation maps with mean June maximum temperatures are given in Figure 8.

In July and August, EOF1 (Figure 7a) is significantly correlated with maximum temperature in all areas of the UK, though correlation values are lower in the far north-

TABLE 3 Summary of significant relationships between the indices and temperature and precipitation.

July/August temperature	June temperature	Winter temperature
Mean temperature, prolonged hot spells and extreme heat positively correlated with EOF1 and EOF2 over much of Britain and Scandinavia. Positively correlated with EOF3 over much of northern half of Europe (but not Britain) and especially Scandinavia. Few areas of significant correlation with jet speed or jet latitude.	Positively correlated with EOF1 over most of Britain (except the south) and Scandinavia. Positively correlated with EOF2 in most parts of Britain, France and Spain. Negatively correlated with EOF3 in western Britain. Areas of significant correlation with EOF1 and EOF2 tend to drop for the latest period (1991–2020) but extreme max temperatures remain strongly correlated with EOF1 in Britain. Jet speed and EOF3 negatively linked with standard deviation in western Britain.	EOF1 and jet speed are both significantly and positively correlated with temperature over most of Europe. EOF3 is negatively correlated with temperature over most of France and Spain. A high jet latitude is linked with low minimum temperatures (but less so low maximum temperatures) in Spain. Standard deviation is negatively linked with EOF1 in Scotland, Ireland and eastern Europe.
July/August precipitation	June precipitation	Winter precipitation
Strong negative correlation between precipitation and EOF1 in Britain and most of Scandinavia and the Netherlands. Negative correlations with very wet days are lower, perhaps reflecting the tendency for anticyclonic spells to have occasional thundery downpours. EOF2 negatively correlated with precipitation in north-western Britain, but this link has declined for the most recent period (1991–2020). Few areas of significant correlation with jet speed or jet latitude.	Precipitation is negatively correlated with EOF1 in most parts of Britain, northern France, the Netherlands and southern Scandinavia. It is negatively correlated with EOF2 in France, southern Britain and parts of Spain, but positively correlated with EOF3 in the west and north-west of Britain. Not many significant correlations with jet speed or jet latitude, but negatively correlated with jet latitude in southern Britain.	EOF1 is positively correlated with winter precipitation in western Britain and most of Scandinavia, and negatively correlated with precipitation in most parts of southern Europe Positive link in western Britain has increased over the time period. EOF2 is positively correlated with winter precipitation in southern Britain and the west of France and Spain. EOF3 is negatively correlated with winter precipitation over a large part of north-west Europe. Jet speed is positively correlated with winter precipitation in most of northern Europe.

west and south-east than elsewhere in the UK. EOF2 (Figure 7b) is correlated with maximum temperature except in north-east Norfolk. This is the one metric that differs substantially from the ERA5-derived results (see Figure S4), for using ERA5, the areas of significant positive correlation with EOF2 were far more confined to north-western Britain. However, as was observed in the ERA5 based analysis, the areas of significant correlation drop substantially for the most recent period (1991–2020). EOF3 is positively correlated with maximum temperature only in north-east Norfolk. When considering prolonged hot weather (as measured by consecutive days over the 80th percentile), all regions see positive correlations with EOF2 as well as EOF1 (not shown). For minimum temperature (not shown), EOF3 is positively linked with minimum temperature in most areas of the UK, but positive correlations with EOF1 and EOF2 are weaker than for maximum temperature, though still significant over large areas of the UK.

In the case of June (Figure 8), EOF1 is positively correlated with maximum temperature over most of the UK, but not in the south and south-east of the country or in the Western Isles. As EOF1 is similar for June and for July/August, a possible reason for the weaker correlation with June maximum temperatures is lower sea surface temperatures in the North Sea and a higher likelihood of cool cloudy weather associated with easterly and north-easterly winds. EOF2 is linked with high maximum temperatures in the east and south of Britain, but not in western Scotland, north-west England, west Wales or Northern Ireland, presumably reflecting the tendency for high SLP centred to the south to result in mainly westerly winds. EOF3 is negatively linked with June maximum temperatures especially in the

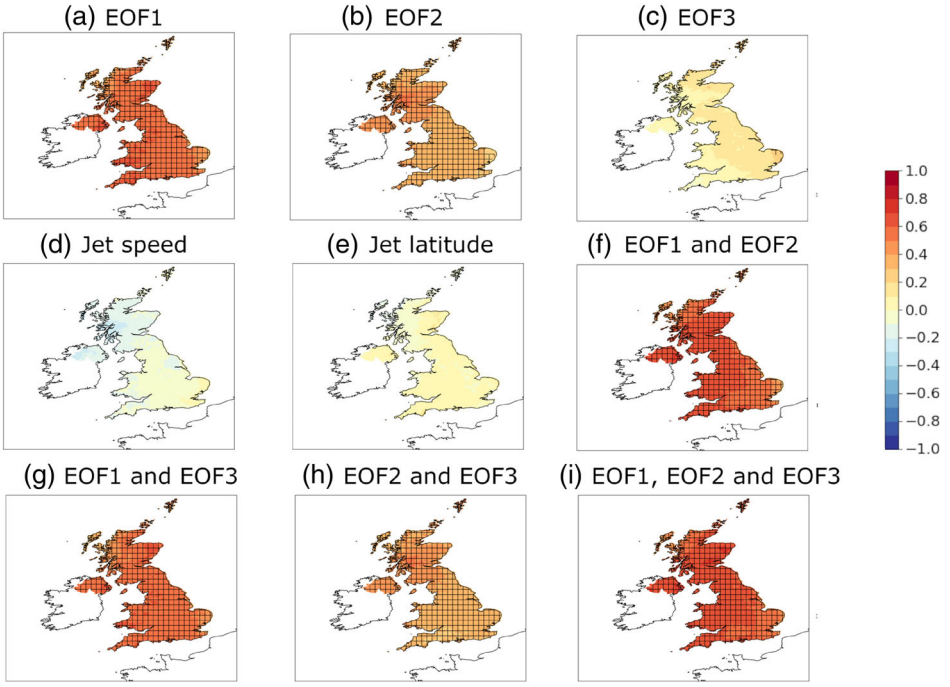

FIGURE 7 Correlations between the three EOFs and July/August maximum temperature above the 90th percentile using HadUK-Grid over the period 1961–2021. Hatched areas indicate correlations that are significant at $p < 0.05$. [Colour figure can be viewed at wileyonlinelibrary.com]

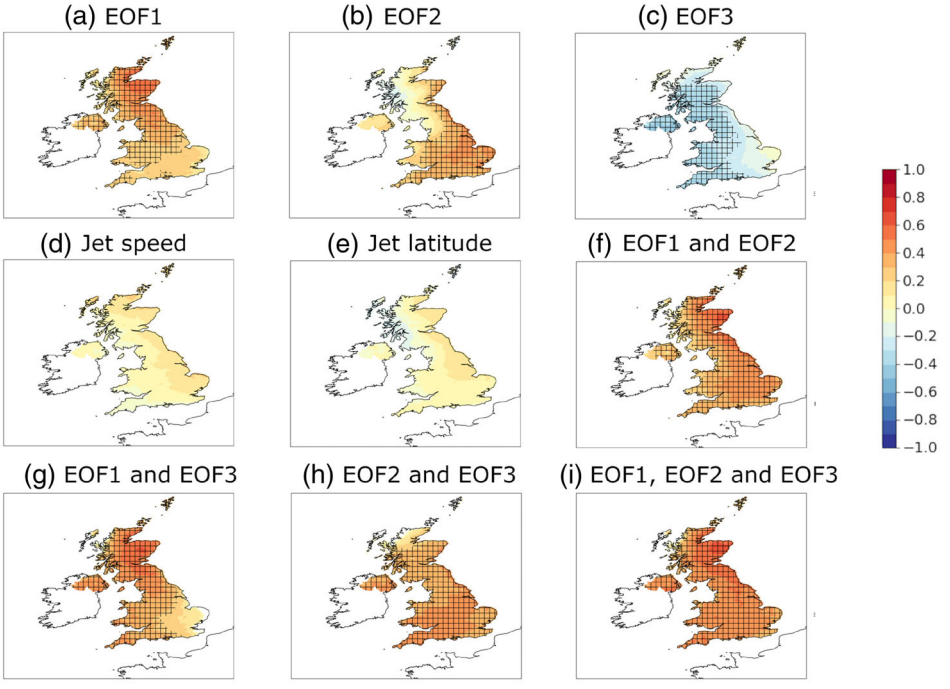

FIGURE 8 Correlations between the three EOFs and June mean maximum temperature using HadUK-Grid over the period 1961–2021. Hatched areas indicate correlations that are significant at $p < 0.05$. [Colour figure can be viewed at wileyonlinelibrary.com]

west of Britain, but not in counties bordering the North Sea. In contrast, areas of positive correlation with June minimum temperature are limited, with some grid boxes in north-west Scotland seeing significant positive correlations between mean minimum temperature and EOF1 (not shown).

4.2.2 | Winter temperature

Correlations between the EOFs, jet speed, jet latitude and winter mean maximum temperatures are shown in Figure S6. As with the ERA5 based analysis, HadUK-Grid analysis of UK winter mean temperature shows strong positive correlations between both maximum and minimum winter temperature and EOF1 (Figure S6a), while correlations with EOF2 and EOF3 are weak, except for some significant positive correlations between EOF3 and winter maximum temperature at some grid boxes in northern Scotland. Correlations between winter maximum and minimum temperatures with the jet speed (Figure S6d) are not significant in north-west Scotland but are significant in other regions of the UK. The

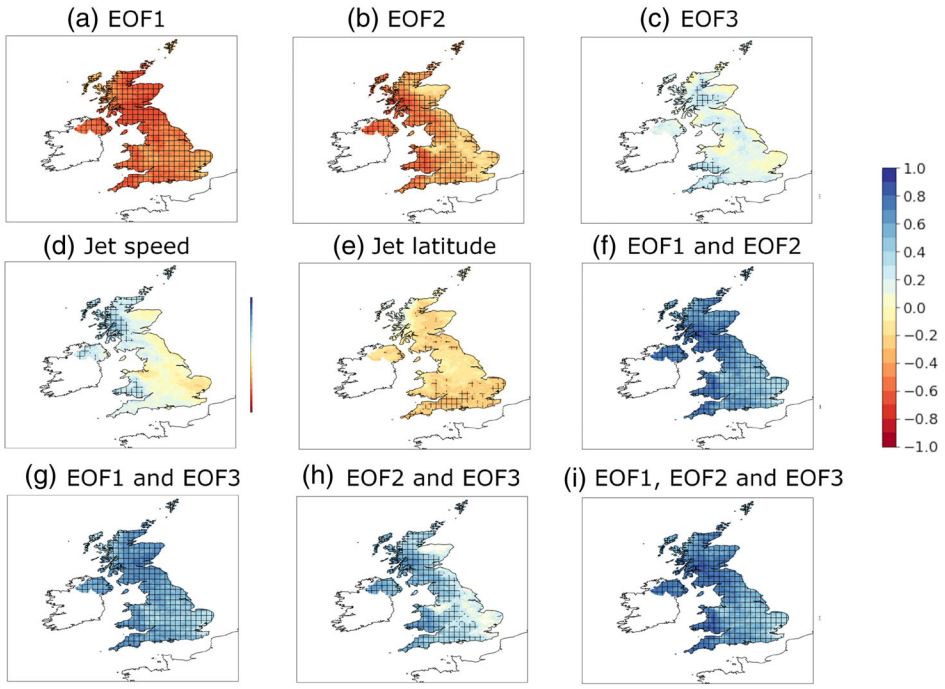

FIGURE 9 Correlations between combinations of the three EOFs and July/August precipitation using HadUK-Grid over the period 1961–2021. Hatched areas indicate correlations that are significant at $p < 0.05$. [Colour figure can be viewed at wileyonlinelibrary.com]

multiple correlation coefficients are, correspondingly, dominated by the positive link with EOF1. The standard deviation of winter temperature (not shown) is negatively linked with EOF1 in south-western Britain, which is consistent with a positive phase of the NAO being linked with reduced temperature variability.

4.2.3 | Summer precipitation

UK high summer (July/August) precipitation (Figure 9) shows more clearly defined local and regional variation using HadUK-Grid than the lower resolution ERA5 reanalysis. EOF1 (Figure 9a) is negatively correlated with precipitation in all areas of the UK. EOF2 (Figure 9b) is also negatively related to precipitation in most regions, but not in parts of north-west Scotland, north-east Scotland and eastern England. There are limited areas of positive correlation between EOF3, mostly in south-west England and central Scotland (Figure 9c). The combination of EOFs 1 and 2 show particularly high correlations with precipitation in central and western Wales and south-west Scotland.

In the case of June (Figure S7), EOFs 1 and 2 both show a northwest-southeast split, but EOF1 is significantly negatively correlated with precipitation in almost all parts of the UK bar north-west Scotland. Negative correlations with EOF2 are limited mainly to southern and eastern Britain, and positive correlations are seen near the west coast of Scotland. EOF3 is positively correlated with precipitation in most of western Scotland, but not elsewhere.

For each of the summer months, precipitation standard deviation is also negatively correlated with EOFs 1 and 2 in most parts of the country (not shown).

4.2.4 | Winter precipitation

Using HadUK-Grid, finer regional detail can be found when comparing atmospheric circulation indices against winter precipitation (Figure 10). EOF1 (Figure 10a) broadly matches previous work by Hall and Hanna (2018), showing significant positive correlations in western Scotland, north-west England and parts of Wales and the West Country, but not in eastern Britain, where small but locally significant negative correlations are seen near the east coast of Scotland and the north-east coast of England. Jet speed is positively linked with mean total winter precipitation except near North Sea coasts from Norfolk northwards, indicating that, taking the UK as a whole, the jet speed is a stronger predictor of wet winters than EOF1.

EOF2 (Figure 10b) is significantly positively correlated with winter precipitation in southern Britain and parts of south-east Scotland and north-east England, while EOF3 (Figure 10c) is negatively correlated with precipitation everywhere except north-west Scotland. Over much of southern England, very wet winters are linked with positive EOF2/negative EOF3 winters, while in north-west Scotland, positive EOF1 winters tend to be very wet, while elsewhere very wet winters are associated primarily with negative values of EOF3. As the last panel

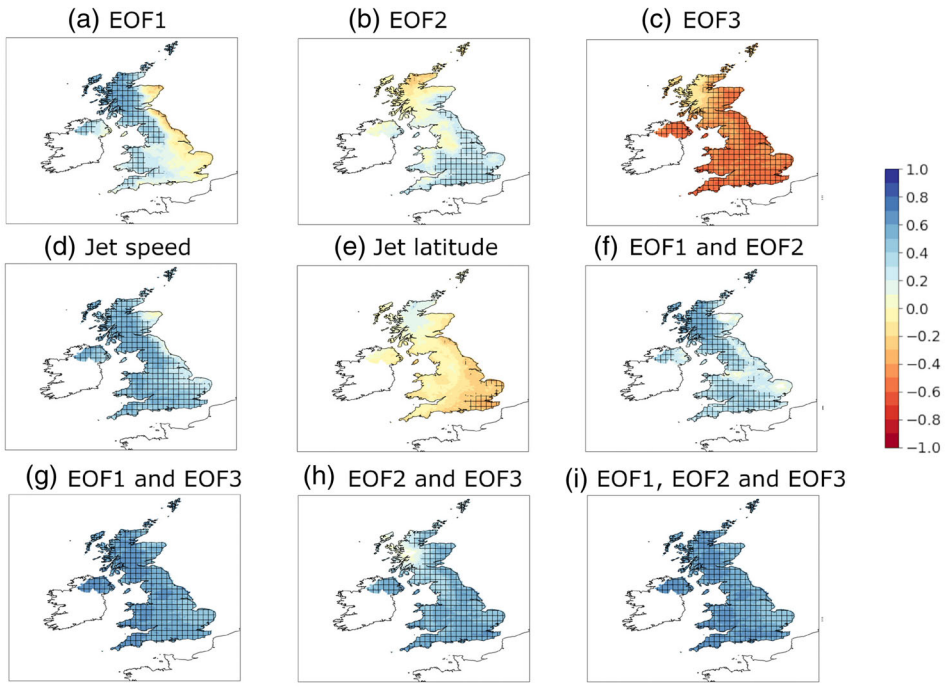

FIGURE 10 Correlations between combinations of the three EOFs, jet speed and latitude and mean total winter precipitation using HadUK-Grid over the period 1961–2021. Hatched areas indicate correlations that are significant at $p < 0.05$. [Colour figure can be viewed at wileyonlinelibrary.com]

of Figure 10 illustrates, the combined multiple correlation coefficient of EOF1, EOF2 and EOF3 is significant in all parts of the UK.

The extremes and persistence indices show very similar relationships with the EOFs, jet speed and jet latitude to mean precipitation (not shown). There is a consistent tendency for correlations with wet winters to be matched by correlations with a high standard deviation (Figure S8), indicating that wetter winters tend to have more variable daily precipitation. This relationship appears to be consistent across all circulation indices. As with the winter precipitation outputs of ERA5 (Figure 6), the HadUK-Grid outputs show a step-change towards more positive correlations between EOF1 and winter precipitation between the periods 1971–2000 and 1981–2010 (not shown).

4.2.5 | Case studies of extreme EOF values and UK temperature and precipitation

Tables 4–6 shows case studies of extreme values of the three EOFs and UK winter and summer temperature and precipitation, based on detrended Met Office national values derived from HadUK-Grid over the period 1961–2021 (corresponding to the period covered in this analysis).

Table 4 shows results for June. The high EOF1 Junes of 1988 and 2006 were very dry, and 2006 was also very warm, which is in line with the results in Section 4, but the third highest value in 1999 was associated with a cool and fairly wet June. The three Junes with the lowest EOF1 were all wet Junes. EOF2 is correlated with a north–south split in June temperature and precipitation anomalies in the UK, which may explain why the three highest EOF2 Junes included a relatively cool June in 1994 and a wet one in 2017 (taking the UK as a whole), as well as the famously hot dry one in 1976 (Baker et al., 2021). The three Junes with the lowest values of EOF2 were in the top 15 wettest. The three Junes with the highest EOF3 values were all on the cool side, while two of the three Junes with the lowest EOF3 values (1995 and 1975) were very dry.

Table 5 shows the extreme EOF years for July/August and corresponding detrended UK temperature and precipitation values. The three highest values of EOF1 were associated with warm and dry high summers, while the three lowest values were associated with wet high summers. Extreme low values of EOF2 were also associated with wet summers, while extreme low values of EOF3 were linked with cool summers. Summer 2009 appears both in the low EOF1 and high EOF3 lists.

For winter (Table 6), all three of the lowest values of EOF1 were associated with cold dry winters, while the winter with the highest value of EOF1 (1988/89) was also clearly the mildest. Although extreme low values of EOF2 were not associated with extreme winters, extreme high values were associated with very wet winters. As would be expected from the strong negative correlations between EOF3 and UK winter precipitation, the three winters with the most extreme negative values of EOF3 were also very wet, and the three with the highest values

TABLE 4 Extreme values of the EOFs and June temperature and precipitation (based on detrended values from the Met Office UK national series over the period 1961–2021).

Value	Year	UK max temp (°C)	Rank (out of 61)	UK min temp (°C)	Rank (out of 61)	UK precip (mm)	Rank (out of 61)
Extreme values of EOF1							
1.77	1988	17.76	25	9.07	21	37.6	58
1.71	2006	19.10	4	9.25	14	39.3	54
1.67	1999	16.53	50	8.01	51	92.3	18
−1.58	1998	16.26	53	8.84	30	120.5	4
−1.90	1982	17.88	22	9.81	6	100.7	12
−2.56	2012	15.48	57	8.21	44	145.1	1
Extreme values of EOF2							
2.68	1994	16.94	40	8.53	39	62.2	37
2.12	1976	20.20	1	10.25	2	41.4	52
1.78	2017	17.88	24	9.90	4	105.6	7
−1.55	1972	14.89	60	7.04	61	96.0	13
−1.62	1997	16.38	51	8.76	33	114.8	5
−2.14	2020	17.72	26	9.13	18	102.2	11
Extreme values of EOF3							
2.34	1990	16.32	52	8.52	40	94.0	15
2.33	1972	14.89	60	7.04	61	96.0	13
1.91	1978	16.76	45	8.50	41	64.4	35
−1.43	1995	17.52	31	8.21	45	29.0	61
−1.62	2019	16.74	47	8.55	37	103.8	9
−2.13	1975	18.72	7	8.07	49	38.7	57

of EOF3 were dry. 2013/14 and 1965/66 appear both in the three highest values of EOF2 and the three lowest values of EOF3.

A limitation of this analysis is that the results in previous sections of this paper indicate that there are regional variations in some cases, especially for precipitation anomalies, which are not captured when examining the UK as a whole. For example, in the case of June, EOF2 is shown to be correlated with warm dry weather in most parts of the UK, but not in western Scotland. The extreme EOF2 June of 1976, which ranks as a top 10 warmest and driest June in most regions of the UK, does not rank in the top 10 for maximum temperature in the Met Office Scotland W region, nor does it rank as substantially drier than average. However, for example, the extreme negative EOF3 winters of 2013/14 was very wet at the opposite regions of the country. A detailed regional breakdown is outside of the scope of this paper, but these UK wide results should be caveated by comparing with the regional variations identified in the HadUK-Grid based correlation analysis.

5 | DISCUSSION

These results suggest that there is considerable potential, given reasonably accurate seasonal forecasts of the three principal EOFs of 500 hPa GPH variability (Sun et al., submitted; Hall et al., 2019), to achieve some skill in predicting the likely seasonal temperature and precipitation anomalies in north-west Europe as well as predicting the atmospheric circulation anomalies.

In winter, EOF1 corresponds closely to the NAO, but with the main low GPH anomaly centred over southern Greenland. The strong positive correlations with temperature over most of Europe, and with precipitation in north-western Britain and western Norway, are consistent with previous findings (e.g., Hurrell & Deser, 2009; Seager et al., 2020). The spatial patterns of correlation between UK winter precipitation and EOF1 are consistent with the findings of Baker et al. (2018), who showed that wet winters in western Scotland are especially strongly linked with a strong mean westerly flow over Britain. Also, the correlation patterns between EOF1 and

TABLE 5 Extreme values of the EOFs and July/August temperature and precipitation (based on detrended values from the Met Office UK national series over the period 1961–2021).

Value	Year	UK max temp (°C)	Rank (out of 61)	UK min temp (°C)	Rank (out of 61)	UK precip (mm)	Rank (out of 61)
Extreme values of EOF1							
2.46	1983	21.75	3	11.77	2	80.9	59
1.86	1976	21.97	2	11.11	10	76.1	60
1.55	2018	20.10	12	10.77	22	123.6	52
−1.88	2019	19.42	17	11.14	9	207.6	11
−2.17	2015	17.95	52	9.75	58	200.2	15
−2.25	2009	18.68	34	10.76	23	251.2	3
Extreme values of EOF2							
1.69	2021	19.06	24	10.79	20	126.0	51
1.45	1968	18.47	38	10.47	34	177.4	25
1.40	2003	20.47	8	11.58	5	99.0	57
−1.30	1985	17.79	54	10.36	40	267.0	2
−1.43	2017	18.14	46	10.05	54	190.5	20
−3.49	1992	18.12	47	10.42	35	249.1	4
Extreme values of EOF3							
1.82	2015	17.95	52	9.75	58	200.2	15
1.71	1997	20.56	7	11.59	4	144.7	42
1.55	2009	18.68	34	10.76	23	251.2	3
−1.33	1993	17.39	60	9.40	61	155.6	37
−1.54	1998	17.98	51	10.21	44	168.4	34
−1.84	1987	18.38	40	10.51	33	174.6	27

UK winter precipitation closely match the correlation patterns with the NAO observed by Stringer et al. (2020). Orographic effects show up in the HadUK-Grid analysis, with EOF1 being positively correlated with winter precipitation in most of western Britain but not in the east, reflecting orographic enhancement in the west and a rain shadow effect in the east. The EOF2 pattern is often linked with a more southerly tracking jet stream, resulting in drier weather over high ground in the north-west. The positive phase of EOF2 is linked with warmer than average winters in southern Europe, and wetter than average winters in France, Spain and southern England, while EOF3 is linked with cold winters in southern Europe and dry winters in north-west Europe. Positive correlations between EOF1 and winter precipitation increased between the periods 1971–2000 and 1981–2010, and stayed at that higher level over 1991–2020, particularly in western Britain, but at the same time they have reduced in northern Scandinavia.

The EOF3 relationships differ from previous studies on the winter Scandinavian pattern (e.g., Bueh & Nakamura, 2007), because the high GPH anomaly of EOF3 is centred over northern Britain and the North Sea rather than Scandinavia, which sends cold easterly winds further south through Europe and does not result in above-average rainfall in south-western Europe. Overall, the findings suggest that cold winters are likely in southern Europe when EOF2 is strongly negative and EOF3 is strongly positive, while cold winters are likely in northern Europe when EOF3 is strongly negative. In Britain, wet winters are most likely when EOF3 is strongly negative. Again, this is consistent with the findings of Baker et al. (2018), where wet winters in most parts of England and in eastern Scotland were shown to be especially correlated with a SLP anomaly pattern that strongly resembles the negative phase of EOF3.

In high summer (July and August), EOF1 has the association with warm and dry weather in Britain and Scandinavia associated with the summer NAO (Folland et al., 2009). All three of the principal EOFs are significantly correlated with summer heat in large areas of northern Europe.

EOF2 corresponds broadly to a form of the East Atlantic pattern with positive GPH anomalies off north-

TABLE 6 Extreme values of the EOFs and winter temperature and precipitation (based on detrended values from the Met Office UK national series over the period 1961 to 2021).

Value	Year	UK max temp (°C)	Rank (out of 61)	UK min temp (°C)	Rank (out of 61)	UK precip (mm)	Rank (out of 61)
Extreme values of EOF1							
1.91	1988/89	8.65	1	3.06	1	319.5	30
1.37	1992/93	6.78	29	1.38	21	312.6	35
1.10	2019/20	7.17	20	1.83	12	428.0	5
−1.82	2010/11	4.72	58	−0.96	58	231.0	54
−1.99	1968/69	5.67	49	0.46	42	300.3	40
−3.24	2009/10	3.91	60	−1.64	60	223.6	56
Extreme values of EOF2							
2.32	1989/90	7.76	6	2.25	6	483.8	3
1.95	2013/14	7.26	15	1.88	11	503.4	1
1.56	1965/66	6.38	35	1.23	23	394.1	11
−1.67	2014/15	6.12	40	0.37	44	326.3	26
−2.20	1980/81	6.90	26	1.06	31	308.5	34
−2.33	2004/05	7.11	21	1.50	18	284.7	45
Extreme values of EOF3							
2.70	1991/92	7.02	23	1.19	28	249.4	51
2.04	1963/64	6.51	32	1.04	32	164.6	61
1.63	1971/72	7.18	17	2.26	5	297.0	41
−2.01	2013/14	7.26	15	1.88	11	503.4	1
−2.01	1965/66	6.38	35	1.23	23	394.1	11
−2.17	2015/16	7.59	7	2.00	9	465.6	4

western Britain. Until the most recent period (1991–2020) it was negatively linked with precipitation in western and north-western Britain, but in 1991–2020 the area of significant negative correlation reduced. This could be related to the southward movement of the jet stream in recent summers and increased blocking over Greenland (Hanna et al., 2015), or to EOF1 having become proportionally more important relative to EOFs 2 and 3 for more recent periods. In Britain EOF3 is most strongly associated with high summer minimum temperatures, while EOF1 is strongly linked with high maximum temperatures in Britain and Scandinavia. The jet speed and latitude are not significantly correlated with temperature and precipitation in summer in most parts of Europe, which may be because the jet stream typically runs further to the north of Europe in summer than in winter.

June has been considered separately. EOF1 for June is similar to EOF1 for July and August, but it is not associated with high summer daytime temperatures in south-eastern Britain, nor with dry weather in north-west Scotland, unlike in July and August. EOF2 for June is a variant of the East Atlantic pattern with above-average geopotential heights covering southern Britain and France and the east Atlantic trough to the west. This produces warm and dry weather in south-eastern Britain and in France, but the westerly and south-westerly winds on the northern flank of the high height anomaly are associated with relatively wet weather in western Scotland. The positive phase of EOF3 is a predominantly cyclonic pattern in north-west Europe with above-average geopotential heights to the north of Scandinavia, resulting in an association with cool and wet weather in western Britain.

As Table 7 indicates, the winter EOFs used in this paper are similar to the EOFs obtained by Dalelane et al. (2020), and both the summer and winter EOFs are similar to those used by Hall and Hanna (2018). However, Dalelane et al. (2020) focused on case studies of European winters, rather than the systematic analysis of correlations between EOFs and temperature and precipitation used in this study. When Golian et al. (2022) derived winter EOFs using MSLP rather than GPH, using the seasonal forecast models GloSea5 and SEAS5, the anomaly patterns were very different from the EOFs

TABLE 7 Other studies that relate European/North Atlantic atmospheric circulation patterns to temperature and/or precipitation anomaly patterns, compared with this study.

Study	Data sources	Time period	Methods	Findings
Scaife et al. (2014)	GloSea5 forecast system, ERA-Interim reanalysis and Forecasting Ocean Assimilation Model	1993–2012	Forecast skill related to correlations with temperature, precipitation, storminess, wind speed	GloSea5 showed significant skill at predicting the winter NAO, which can be related to surface weather
Hall and Hanna (2018)	SLP data from NCEP/NCAR reanalysis	1951–2016	Three principal EOFs derived from 20CRv2 reanalysis, 1951–2014	Three EOFs useful for predicting UK winter and summer temperature and precipitation
Dobrynin et al. (2018)	MPI-ESM-MR seasonal prediction system, using ERA-Interim reanalysis	1982–2016	Providing a 'first guess' method of predicting the NAO from the initial state of the ocean, sea ice, land and stratosphere	Predictability of the winter NAO increased to 0.83 when using these combined methods
Dalelane et al. (2020)	German Climate Forecast System (GCFS 2.0) and MiKlip decadal prediction system	1990–2017 (GCFS), 1958–present (MiKlip)	Prediction systems nudged with ERA40, ERA-INTERIM and NSIDC Arctic sea ice, looking at three other winter patterns besides the NAO	Increased prediction skill of wintertime mean sea level pressure, surface temperature and precipitation over Europe
Seager et al. (2020)	ERA-Interim reanalysis used for precipitation and 500 hPa heights, compared with NOAA CPC merged analysis of precipitation	1979–2017	NAO given as first EOF of DJFM seasonal mean 500 hPa heights, regressed against ERA-Interim to get relation with precipitation	Winter precipitation anomalies in NW Europe + Mediterranean mostly governed by mean flow anomalies
Golian et al. (2022)	Hindcasts of mean sea level pressure from GloSea5 and SEAS5 for winter (DJF) and summer (JJA). MSLP data based on ERA5 reanalysis	1950–2019 for ERA5, 1993–2016 for GloSea5 and SEAS5 model hindcasts	Multiple linear regression and neural network AI applied to four Irish rainfall regions	Leveraging information about MSLP from dynamical systems assists Irish precipitation forecasts for summer and winter
This study	Detrended ERA5 500 hPa geopotential height, ERA5 temperature and precipitation data, HadUKGrid temperature and precipitation for the UK	1951–2021	Python EOFs package used to generate three principal component EOFs (corresponding to NAO, EA and SCA) and multiple linear regression	Results based on UK as well as Europe show that three principal EOFs are linked with temperature and precipitation

obtained here, suggesting that the EOFs that are generated can be sensitive to the methodology used. Ural blocking is known to influence surface weather conditions, especially via the Warm Arctic Cold Siberia pattern (Tyrlis et al., 2020), but this pattern only showed up as EOF4 in our study, accounting for 9.5% of winter variability.

A further aim is to be able to use probabilistic predictions of the NAO, EA and SCA using Nonlinear Auto-Regressive Moving Average with eXogenous inputs (NARMAX) machine learning models to forecast likely temperature and precipitation anomalies and variability in north-west Europe. Previous research (Sun et al., submitted; Hall et al., 2019) has suggested that with the

aid of NARMAX, it is possible to predict each of the three principal EOFs with some skill for winter, June and July/August, whereas dynamical models have so far struggled to show skill in predicting anything other than the winter NAO and EA (Sun et al., submitted).

One issue with using EOF analysis is non-stationaries, where the main SLP and GPH anomaly centres shift positions over time as the relationships between meteorological variables and atmospheric circulation patterns change (Huth & Beranová, 2021), and station-based versions of the summer NAO are not well correlated with summertime UK temperature or precipitation (Hall & Hanna, 2018). Thus, there is also a strong argument for providing seasonal forecasts of jet speed and jet latitude. However, our results suggest that jet speed and jet latitude alone may not account for much of the variability in temperature and precipitation in some cases. For example, Figure 2 showed that in northern Europe, July/August temperatures and extremes are positively correlated with each of the three EOFs over large areas, but they are not significantly correlated with jet speed or jet latitude in most parts of Europe. This suggests that using jet speed and jet latitude is not sufficient to determine temperature and precipitation variability in most parts of Europe, especially in summer, and that using the EOFs in addition is important.

6 | SUMMARY

These results show the first three principal component EOFs of circulation variability, together with jet speed and jet latitude, are significantly correlated with temperature and precipitation over much of Europe, and that some of the variability cannot be explained by the NAO alone (which corresponds closely to EOF1 in each of the cases studied here). For central and northern Europe as a whole, EOF1 is by far the dominant index for predicting temperature variability in winter, and the summer EOF1 is strongly linked with below-average precipitation in most parts of north-west Europe, especially Britain and Scandinavia. However, for north-west Europe, EOF3 (corresponding to a westward displaced Scandinavian pattern with the high GPH anomaly over northern Britain and the North Sea) is most strongly linked with winter precipitation. In July and August, all three of the first three principal component EOFs showed significant correlations with high temperatures in large areas of northern Europe. These are consistent with but substantially extend the findings of Hall and Hanna (2018) specifically regarding the UK. The different, and in many cases significant, results for June and July/August also suggest that there is scope for achieving more detailed results by breaking seasonal forecasts down into individual months.

AUTHOR CONTRIBUTIONS

Ian Simpson: Writing – original draft; methodology; validation; visualization; investigation; writing – review and editing; conceptualization; software; data curation. **Edward Hanna:** Project administration; supervision; resources; funding acquisition; conceptualization; writing – review and editing; methodology. **Laura Baker:** Writing – review and editing. **Yiming Sun:** Writing – review and editing. **Hua-Liang Wei:** Writing – review and editing.

ACKNOWLEDGEMENTS

We acknowledge NERC for funding this research (grant NE/V001787/1), the ECMWF for providing the ERA-5 reanalysis (via Copernicus) and the UK Met Office National Climate Information Centre for providing HadUK-Grid. We also thank Len Shaffrey for helpful comments, and Richard Hall and Thomas Cropper for useful feedback and advice on generating the three principal EOFs.

DATA AVAILABILITY STATEMENT

The data that support the findings of this study are available from the corresponding author upon reasonable request.

ORCID

Ian Simpson https://orcid.org/0009-0004-5525-9287
Edward Hanna https://orcid.org/0000-0002-8683-182X
Laura Baker https://orcid.org/0000-0003-0738-9488

REFERENCES

Baker, L., Shaffrey, L. & Hawkins, E. (2021) Has the risk of a 1976 north-west European summer drought and heatwave event increased since the 1970s because of climate change? *Quarterly Journal of the Royal Meteorological Society*, 147(741), 4143–4162. Available from: https://doi.org/10.1002/qj.4172

Baker, L.H., Shaffrey, L.C. & Scaife, A.A. (2018) Improved seasonal prediction of UK regional precipitation using atmospheric circulation. *International Journal of Climatology*, 38, e437–e453. Available from: https://doi.org/10.1002/joc.5382

Barnston, A.G. & Livezey, R.E. (1987) Classification, seasonality and persistence of low-frequency atmospheric circulation patterns. *Monthly Weather Review*, 115, 1083–1126. Available from: https://doi.org/10.1175/1520-0493(1987)115<1083:CSAPOL>2.0.CO;2

Bueh, C. & Nakamura, H. (2007) Scandinavian pattern and its climatic impact. *Quarterly Journal of the Royal Meteorological Society*, 133, 2117–2131. Available from: https://doi.org/10.1002/qj.173

Cohen, J., Coumou, D., Hwang, J., Mackey, L., Orenstein, P., Totz, S. et al. (2019) S2S reboot: an argument for greater

inclusion of machine learning in subseasonal to seasonal forecasts. *Wiley Interdisciplinary Reviews: Climate Change*, 10, e00567. Available from: https://doi.org/10.1002/wcc.567

Dalelane, C., Dobrynin, M. & Fröhlich, K. (2020) Seasonal forecasts of winter temperature improved by higher-order modes of mean sea level pressure variability in the North Atlantic sector. *Geophysical Research Letters*, 47, e2020GL088717. Available from: https://doi.org/10.1029/2020GL088717

Dawson, A. (2016) Eofs: a library for EOF analysis of meteorological, oceanographic, and climate data. *Journal of Open Research Software*, 4(1), e14. Available from: https://doi.org/10.5334/jors.122

Dobrynin, M., Domeisen, D.I.V., Müller, W.A., Bell, L., Brune, S., Bunzel, F. et al. (2018) Improved teleconnection-based dynamical seasonal predictions of boreal winter. *Geophysical Research Letters*, 45, 3605–3614. Available from: https://doi.org/10.1002/2018GL077209

Folland, C.K., Knight, J., Linderholm, H.W., Fereday, D., Ineson, S. & Hurrell, J.W. (2009) The summer North Atlantic Oscillation: past, present, and future. *Journal of Climate*, 22, 1082–1103. Available from: https://doi.org/10.1175/2008JCLI2459.1

Golian, S., Murphy, C., Wilby, R.L., Matthews, T., Donegan, S., Quinn, D.F. et al. (2022) Dynamical–statistical seasonal forecasts of winter and summer precipitation for the Island of Ireland. *International Journal of Climatology*, 42(11), 5714–5731. Available from: https://doi.org/10.1002/joc.7557

Haiden, T. & Trentmann, J. (2015) Verification of cloudiness and radiation forecasts in the greater Alpine region. *Meteorologische Zeitschrift*, 25, 3–15. Available from: https://doi.org/10.1127/metz/2015/0630

Hall, R., Erdelyi, R., Hanna, E., Jones, J.M. & Scaife, A.A. (2015) Drivers of North Atlantic polar front jet stream variability. *International Journal of Climatology*, 35, 1697–1720. Available from: https://doi.org/10.1002/joc.4121

Hall, R.J. & Hanna, E. (2018) North Atlantic circulation indices: links with summer and winter UK temperature and precipitation and implications for seasonal forecasting. *International Journal of Climatology*, 38, e660–e677. Available from: https://doi.org/10.1002/joc.5398

Hall, R.J., Wei, H.-L. & Hanna, E. (2019) Complex systems modelling for statistical forecasting of winter North Atlantic atmospheric variability: a new approach to North Atlantic seasonal forecasting. *Quarterly Journal of the Royal Meteorological Society*, 145, 2568–2585. Available from: https://doi.org/10.1002/qj.3579

Hanna, E., Cropper, T.E., Jones, P.D., Scaife, A.A. & Allan, R. (2015) Recent seasonal asymmetric changes in the NAO (a marked summer decline and increased winter variability) and associated changes in the AO and Greenland Blocking Index. *International Journal of Climatology*, 35, 2540–2554. Available from: https://doi.org/10.1002/joc.4157

Hardiman, S.C., Dunstone, N.J., Scaife, A.A., Smith, D.M., Knight, J.R., Davies, P. et al. (2020) Predictability of European winter 2019/20: Indian Ocean dipole impacts on the NAO. *Atmospheric Science Letters*, 21, e1005. Available from: https://doi.org/10.1002/asl.1005

Hersbach, H., Bell, B., Berrisford, P., Hirahara, S., Horányi, A., Muñoz-Sabater, J. et al. (2020) The ERA5 global reanalysis. *Quarterly Journal of the Royal Meteorological Society*, 146, 1999–2049. Available from: https://doi.org/10.1002/qj.3803

Hollis, D., McCarthy, M.P., Kendon, M., Legg, T. & Simpson, I. (2019) HadUK-Grid—A new UK dataset of gridded climate observations. *Geoscience Data Journal*, 6, 151–159. Available from: https://doi.org/10.1002/gdj3.78

Huntingford, C., Marsh, T., Scaife, A., Kendon, E.J., Hannaford, J., Kay, A.L. et al. (2014) Potential influences on the United Kingdom's floods of winter 2013/14. *Nature Climate Change*, 4, 769–777. Available from: https://doi.org/10.1038/nclimate2314

Hurrell, J.W. & Deser, C. (2009) North Atlantic climate variability: the role of the North Atlantic oscillation. *Journal of Marine Systems*, 78, 28–41. Available from: https://doi.org/10.1016/j.jmarsys.2008.11.026

Hurrell, J.W., Kushnir, Y., Ottersen, G. & Visbeck, M. (2003) An overview of the North Atlantic oscillation. In: Hurrell, J.W., Kushnir, Y., Ottersen, G. & Visbeck, M. (Eds.) *The North Atlantic Oscillation: climatic significance and environmental impact*. Washington: American Geophysical Union. Available from: https://doi.org/10.1029/134GM01

Huth, R. & Beranová, R. (2021) How to recognize a true mode of atmospheric circulation variability. *Earth and Space Science*, 8, e2020EA001275. Available from: https://doi.org/10.1029/2020EA001275

Ineson, S. & Scaife, A. (2009) The role of the stratosphere in the European climate response to El Niño. *Nature Geoscience*, 2, 32–36. Available from: https://doi.org/10.1038/ngeo381

Karl, T.R., Nicholls, N. & Ghazi, A. (1999) CLIVAR/GCOS/WMO workshop on indices and indicators for climate extremes: workshop summary. *Climatic Change*, 42, 3–7.

Kendon, M., McCarthy, M., Jevrejeva, S., Matthews, A., Sparks, T., Garforth, J. et al. (2022) State of the UK climate 2021. *International Journal of Climatology*, 42(Supplement 1), 1–80. Available from: https://doi.org/10.1002/joc.7787

MacLachlan, C., Arribas, A., Peterson, K.A., Maidens, A., Fereday, D., Scaife, A.A. et al. (2015) Global seasonal forecast system version 5 (GloSea5): a high-resolution seasonal forecast system. *Quarterly Journal of the Royal Meteorological Society*, 141, 1072–1084. Available from: https://doi.org/10.1002/qj.2396

Peterson, T.C., Folland, C., Gruza, G., Hogg, W., Mokssit, A. & Plummer, N. (2001) Report on the activities of the working group on climate change detection and related rapporteurs 1998-2001. WMO report. WCDMP-47, WMO-TD 1071, Geneve, Switzerland, 143pp.

Scaife, A.A., Arribas, A., Blockley, E., Brookshaw, A., Clark, R.T., Dunstone, N. et al. (2014) Skillful long-range prediction of European and North American winters. *Geophysical Research Letters*, 41, 2514–2519. Available from: https://doi.org/10.1002/2014GL059637

Seager, R., Liu, H., Kushnir, Y., Osborn, T.J., Simpson, I.R., Kelley, C.R. et al. (2020) Mechanisms of winter precipitation variability in the European–Mediterranean region associated with the North Atlantic Oscillation. *Journal of Climate*, 33, 7179–7196. Available from: https://doi.org/10.1175/JCLI-D-20-0011.1

Stringer, N., Knight, J. & Thornton, H. (2020) Improving meteorological seasonal forecasts for hydrological modeling in

European winter. *Journal of Applied Meteorology and Climatology*, 59, 317–332. Available from: https://doi.org/10.1175/JAMC-D-19-0094.1

Sun, Y., Simpson, I.R., Wei, H.-L. & Hanna, E. (submitted) Probabilistic seasonal forecasts of North Atlantic atmospheric circulation using complex systems modelling and comparison with dynamical models. Awaiting publication.

Thornton, H.E., Smith, D.M., Scaife, A.A. & Dunstone, N.J. (2023) Seasonal predictability of the East Atlantic pattern in late autumn and early winter. *Geophysical Research Letters*, 50, e2022GL100712. Available from: https://doi.org/10.1029/2022GL100712

Tyrlis, E., Bader, J., Manzini, E., Ukita, J., Nakamura, H. & Matei, D. (2020) On the role of Ural blocking in driving the warm Arctic–cold Siberia pattern. *Quarterly Journal of the Royal Meteorological Society*, 146, 2138–2153. Available from: https://doi.org/10.1002/qj.3784

Woollings, T. (2010) Dynamical influences on European climate: an uncertain future. *Philosophical Transactions of The Royal Society A Mathematical Physical and Engineering Sciences*, 368, 3722–3756. Available from: https://doi.org/10.1098/rsta.2010.0040

Woollings, T. & Blackburn, M. (2012) The North Atlantic jet stream under climate change and its relation to the NAO and EA patterns. *Journal of Climate*, 25, 886–902. Available from: https://doi.org/10.1175/JCLI-D-11-00087.1

SUPPORTING INFORMATION

Additional supporting information can be found online in the Supporting Information section at the end of this article.

How to cite this article: Simpson, I., Hanna, E., Baker, L., Sun, Y., & Wei, H.-L. (2024). North Atlantic atmospheric circulation indices: Links with summer and winter temperature and precipitation in north-west Europe, including persistence and variability. *International Journal of Climatology*, 1–21. https://doi.org/10.1002/joc.8364